The following article appeared in Journal of Nanomaterials, Volume 2019, Article ID 9846729; and may be found at: 10.1155/2019/2728786

Hindawi
Journal of Nanomaterials
Volume 2019, Article ID 9846729, 11 pages
https://doi.org/10.1155/2019/9846729

Research Article

Plasmonic Sensing of Aqueous-Divalent Metal Ions by Biogenic Gold Nanoparticles

Luisa E. Silva-De Hoyos,[1] **Victor Sánchez-Mendieta**,[1,2] **Alfredo R. Vilchis-Nestor**,[2] **Miguel A. Camacho-López**,[3] **Jésica Trujillo-Reyes**,[4] **and Miguel Avalos-Borja**[5]

[1]*Universidad Autónoma del Estado de México, Facultad de Química, Paseo Colón y Paseo Tollocan, Toluca, Estado de México 50120, Mexico*
[2]*Centro Conjunto de Investigación en Química Sustentable UAEM-UNAM, Carretera Toluca-Ixtlahuaca Km. 14.5, Tlachaloya, Toluca, Estado de México, Mexico*
[3]*Universidad Autónoma del Estado de México, Laboratorio de Fotomedicina, Biofotónica y Espectroscopia Láser de Pulsos Ultracortos, Facultad de Medicina, Toluca, Estado de México 50120, Mexico*
[4]*Department of Chemistry, The University of Texas at El Paso, 500 West University Ave., El Paso, TX 79968, USA*
[5]*Instituto Potosino de Investigación Científica y Tecnológica (IPICyT), División de Materiales Avanzados, San Luis Potosí, Mexico*

Correspondence should be addressed to Victor Sánchez-Mendieta; vsanchezm@uaemex.mx
and Alfredo R. Vilchis-Nestor; arvilchisn@uaemex.mx

Received 20 September 2018; Revised 23 November 2018; Accepted 27 November 2018; Published 17 February 2019

Academic Editor: Ilaria Fratoddi

The chemical interaction between biogenic gold nanoparticles (AuNPs) and several metal (II) ions can be regarded as a practical, twofold, colorimetric, and plasmon resonance sensing method for the recognition of some divalent metal ions in aqueous solutions. The green synthesized AuNPs, using *Camellia sinensis* as a reducing agent, were characterized by a surface plasmon resonance (SPR) using UV-Vis spectroscopy, infrared spectroscopy, and transmission electron microscopy. The AuNP colloidal solutions obtained have a pink-reddish color with SPRs centered between 529 and 536 nm. AuNPs with spherical, triangular, and hexagonal shapes were found by TEM analyses. Despite their divergent morphologies, these AuNPs can be employed as colorimetric and plasmon resonance sensors for detection of Ca^{2+}, Sr^{2+}, Cu^{2+}, and Zn^{2+}, primarily, in aqueous solutions. Sensibility studies based on molar concentrations were also performed for these metal ions. Furthermore, solid biogenic AuNPs/cellulosic biocomposites were prepared with the aim of developing portable, fast, and dependable colorimetric sensors; nevertheless, these biocomposites resulted to be good adsorbent materials of metal ions.

1. Introduction

Divalent metal ions are responsible for the accomplishment of a great number of biological reactions in live organisms. However, depending on their concentration, many of these metal ions, and also in complex compounds, represent hazardous conditions for humans and other live species. Therefore, increasing interest to develop facile, trustworthy, and inexpensive methods for the detection of metal ions has been noticed since the past decade. Nanomaterials are materials where one or more external dimensions are in the range of 1–100 nm [1]. Thus, it has been demonstrated that nanomaterials have unique physical and chemical properties, which have promoted the advent of nanotechnology since about two decades ago [2]. It has also been proved that nanomaterials are not only man-made since there are several of these materials that are formed naturally and coexist in the environment [3]. As part of the nanomaterials, nanoparticles (NPs) are considered particles with a range of sizes between 1 and 100 nm; these nanostructures exhibit improved properties as compared to the bulk-size material; one of the enhanced properties is the optical properties; these can be

modulated by controlling the size, shape, and chemical environments [4]. NPs of noble metals, such as gold and silver, have a great interest in science and technology as they exhibit strong absorption of electromagnetic waves in the visible region of the spectrum due to the surface plasmon resonance (SPR), chemical inertness (AuNPs), stable dispersions (AuNPs), chemical ambient, and biocompatibility (AuNPs). If there is a slight change in the NPs like the size, shape, surface nature, or distance between particles, it can lead to changes in their optical properties. Among the noble metal nanoparticles, gold and silver nanoparticles are perhaps the most studied, due to the relatively easy synthesis methods and to their inherent chemical and optical properties [5, 6]. Thus, these particles can be used in applications such as fabrication of optical devices, surface-enhanced Raman scattering, bioimaging, colorimetric sensors, localized surface plasmon sensing, and fluorescence-enhanced sensors [7]. Localized surface plasmon resonance (LSPR) is known as collective oscillations of free electrons in confined metal systems that require excitations by external electromagnetic waves [8–12]; this happens on extended metal surfaces. LSPR frequencies depend on the size, shape, composition, dielectric constant, and interparticle distance of the NPs [8–14]. Because of these characteristics, NPs are suitable for sensing applications [15]. Due to these relevant applications, researchers around the world seek environmentally friendly process for the synthesis of NPs such as biological methods using microorganisms, plants, or plant extracts. The use of these methods is an alternative to chemical and physical methods. Using plant extracts, the synthesis is carried out extracellularly, the process is relatively easy, and the cost decreases. It is important to mention that the plant extracts contain polyphenols that exhibit the ability of reducing and capping agents [4]. The polyphenols have hydroxyl as well as carboxylic acid groups that play a key role in biosynthesis. Previous studies reported that molecules with two vicinal hydroxyl groups act as reducing agents [16]; in contrast, the role of the carboxylic moiety is to stabilize the nanoparticle as a capping agent, so this group has influence on the control of the shape and size of the metal nanoparticles. Thus, the *Camellia sinensis* aqueous extract with 59.8 ± 1.8 g of total polyphenols, among them, catechol and epicatechin, was highlighted as a biogenic reaction medium to obtain Ag and Au nanoparticles with good control of the morphology and narrower size distribution in contrast to other biosynthetic methods [17–19]. Colorimetric sensing is due to the aggregation of AuNPs with different sizes; this aggregation induces interparticle surface plasmon coupling, resulting in a visible color change from pink to purple. The color change during the aggregation of the NPs provides a way to target different analytes [20]. In this particular work, the type of sensing used is molecular recognition by aggregation; when two NPs are close to each other, they become optically coupled due to the interaction and exhibit an additional resonance. Depending on the proximity between the NPs, the SPR has different changes that leads to a redshift and a color change [13, 21–23]. The extent of the redshift in the SPR depends on the concentration of the metal ions in the solution. The bathochromic shift (red shift) in the SPR band is attributed to the formation of smaller aggregates in the presence of metal ions. When two NPs are close to each other, their SPR is coupled and the new position of the resonance band depends on the number of NPs and their proximity [8, 13, 21–23]. Thanks to the optical properties of the NPs, already mentioned, the use of these for the detection of metal ions in water is a viable and relatively simple method for this application [7, 24–29]. Furthermore, nanoplasmonic devices are known as nanoparticles with plasmonic properties that impregnate solid substrates that can be used in sensing applications. There are a variety of substrates that can be used to immobilize plasmonic nanoparticles such as glass, quartz, silicon, and flexible subtracts such as paper. Also, a diversity of methods can be used to immobilize the nanoparticles on the substrate; in this work, the "dip-coating" method was used to prepare a NPs/cellulosic material composite. Paper or other cellulosic material has been used as a flexible support material, such as supercapacitors and electronic and sensing devices. Some of the advantages are easy fabrication, relatively cheap material, ecofriendly, and biodegradable [30].

In this research, biogenic AuNPs were synthesized using a simple one-pot methodology with *Camellia sinensis* (green tea) extract, as a reducing and capping agent. These AuNP colloidal solutions were used as colorimetric and plasmon resonance sensors of different divalent metal ions in aqueous solution: Mg^{2+}, Ca^{2+}, Sr^{2+}, Cu^{2+},Zn^{2+}, Hg^{2+}, and Pb^{2+}. In addition, AuNPs/cellulosic material composites were prepared and tested as potential portable-metal ion sensor.

2. Experiments

2.1. Materials. *Camellia sinensis* (green tea) was obtained from a local store. $HAuCl_4$, $CaCl_2$, $CuCl_2$, $PbCl_2$, $ZnCl_2$, $SrCl_2$, $HgCl_2$, and $MgCl_2$ were acquired as analytical-grade reagents from Sigma-Aldrich. All chemicals were used without further purification, and deionized water was employed on the synthesis and on the sensing experiments. Cellulosic material (Whatman filter paper) was employed as support for the preparation of AuNPs/cellulosic material composites.

2.2. Preparation of Camellia sinensis Aqueous Extract. 1 g of commercial green tea (Lagg's) was boiled for 20 min in 90 mL of deionized water; upon cooling, the infusion was vacuum filtered. The resulting extract was stored for a day on a flask at room temperature and used as a reducing and capping agent [31].

2.3. Biosynthesis of AuNPs. The biosynthesis of AuNPs was carried out using 5 mL of 10^{-3} M of $HauCl_4$ solution and 0.4 mL of *Camellia sinensis* extract. The synthesis performed was an adaptation of a method previously reported by us [31].

2.4. Characterization of AuNPs. The characterization of AuNPs was carried out by the UV-Vis spectroscopy, using a Lambda 650 Perkin-Elmer spectrophotometer. For transmission electron microscopy (TEM) analyses, the samples were prepared by placing drops of the reaction mixture over carbon-coated grids and allowing evaporation. TEM

observations were performed on a JEOL 2100 microscope operated at accelerating voltage of 200 kV with a LaB_6 filament. To know the amount and shape of the NPs in one sample, approximately 400 NPs per sample were taken into account. Particle size diameters were calculated with the equation $d_{avg} = P(n_i d_i)/Pn_i$, where n_i is the number of particles of diameter d_i.

2.5. Infrared Spectroscopy (FTIR) Analyses. An aliquot of 40 mL *Camellia sinensis* extract and of the biogenic AuNps was, separately, left to dry at room temperature for 48 h. The powders obtained were analyzed from 4000 to 500 nm by using a Bruker spectrophotometer Tensor 27 with MIR source, ATR accessory (model ATR Platinum), and diamond crystal.

2.6. Preparation of AuNPs/Cellulosic Material Composites. The biocomposites were obtained through the in situ bioreduction of $HAuCl_4$, using the *Camellia sinensis* extract, in the presence of a piece of the cellulosic material. Rectangles of 5 cm × 10 cm of filter paper were deposited in a vial with 5 mL of 10^{-3} M $HAuCl_4$ and 0.4 mL of *Camellia sinensis* extract; the mix was left standing for 4 h. After that time, the piece of paper was taken out from the solution and air-dried at room temperature.

2.7. Characterization of AuNPs/Cellulosic Material Composites. The AuNPs/cellulosic material composites were analyzed by UV-Vis diffuse reflectance spectroscopy (DRS UV-Vis) using a Lambda 35 spectrophotometer of Perkin-Elmer. The spectrum of the cellulosic support was subtracted from the spectra of the Au/biocomposites. Environmental scanning electron microscopy (ESEM) was used to evaluate the morphology of the cellulosic fibers modified with Au nanoparticles before and after the sensing studies using a FEI Quanta FEG 250 microscope. Chemical mapping was performed using an EDS spectroscope from EDAX, attached to the FEG 250 equipment.

2.8. Sensing Studies. Sensing experiments were performed with AuNPs prepared with 0.4 mL of reducing agent at room temperature. 1 mL of 10^{-3} M solutions of $CaCl_2$, $CuCl_2$, $PbCl_2$, $ZnCl_2$, $SrCl_2$, $HgCl_2$, and $MgCl_2$ was added, separately, to 1 mL of the AuNP solution at room temperature. To carry out the study of sensibility of the AuNPs towards detection of the metal ions, different concentrations of each one of these ions: 10^{-3}, 10^{-4}, 10^{-5}, and 10^{-6} M, were added to the AuNP solution. The sensing and selectivity of the metal ions by the AuNP solution were analyzed by UV-Vis using a Lambda 650 Perkin-Elmer spectrophotometer.

The solid biocomposites were put in contact with 1 mL of 10^{-3} M metal ion solutions. The solid biocomposites were analyzed by UV-Vis using a Lambda 35 of Perkin-Elmer with an integrated sphere, with a resolution of 1 nm, from 300 to 700 nm.

3. Results and Discussion

3.1. Synthesis and Characterization of AuNPs. Camellia sinensis extract contains various polyphenols: flavonoids (catechol, epicatechin, and caffeine) and phenolic acids (3,4-dihydroxybenzoic acid, vanillic acid, 4-hydroxy-3,5--dimethoxybenzoic acid, and benzoic acid). These components contribute to the antioxidant activities of the extract. The aqueous extract contains 59.8 ± 1.8 (mg of CAE/g dw) total phenols with an antioxidant capacity of 70.1 ± 2.4 (%) [17–19, 32].

The addition of *Camellia sinensis* extract (0.4 mL) to a 10^{-3} M $HAuCl_4$ solution led to the appearance of a dark pink color in the solution after 0.5 h of reaction, indicating the formation of AuNPs and the excitation of SP vibration in the NPs (Figure 1(b)). The colloidal solution resulting from the previous experiment was examined by the UV-Vis spectroscopy. Figure 1 shows the characteristic AuNP SPR bands centered between 529 and 536 nm (Figure 1(a)).

The kinetics of the formation of AuNPs was followed by the UV-Vis spectroscopy (Figure 1(a)); it is observed that with the progress of the reaction, the intensity of the signal at about 536 nm increases with the time of reaction, while a new SPR band centered at around 529 nm appears at about 24 h of reaction (Figure 1(a) violet curve). With a longer time of reaction, the main absorption wavelength undergoes a blue shift before stabilizing at 24 h (Figure 1(a) curve from 0.5 to 24 h). These time-dependent features on the spectra are characteristics of size and shape changes on the AuNPs.

Figures 2(a) and 2(b) show representative transmission electron microscopy (TEM) images of the AuNPs synthesized with 0.4 mL of *Camellia sinensis* extract at room temperature. Different shapes of the biogenic AuNPs: spherical (82%), triangular (14%), and hexagonal (1%), can be seen. TEM analyses reveal the formation of AuNPs with triangular shapes (Figure 2(b)), with an average lateral size of 50 nm, and also particles with spherical shapes (Figure 2(a)), with an average size of 18 nm.

AuNPs obtained with 0.4 mL of *Camellia sinensis* extract show a single crystalline nature of metallic gold as revealed in the selected area electron diffraction rings (SAED) (Figure 2(b), inset). These rings could be indexed as a face-centered cubic (FCC) crystalline phase, assigning the family of planes as {111}, {200}, {220}, and {311}, respectively [33]. With this analysis, we know that the triangles are highly [111] oriented (Figure 2(a) inset).

The *Camellia sinensis* extract and the biogenic AuNPs were characterized by FITR spectroscopy (Figures 3(a) and 3(b)). With these studies, we can confirm the presence of polyphenolic biomolecules on the extract and their interaction with the NP surface. The major constituents of *Camellia sinensis* extract are caffeine, epicatechin, and benzoic acid among others (59.8 ± 1.8 (mg of CAE/g dw) of total polyphenols). These components are associated with the antioxidant activity (70.1 ± 2.4 (%)).

IR bands centered at 3395, 1654, 1639, and 1323 cm^{-1} on *Camellia sinensis* extract are characteristics of the -OH, C=O, and C-O groups, respectively, stretching modes of the carboxylic acid present on the biomolecules. Bands centered at 1654 and 1639 cm^{-1} can be attributable to C=O stretch of the carboxylic acid moiety, except for the presence of the bands centered at 2924 and 2856 cm^{-1}, which may

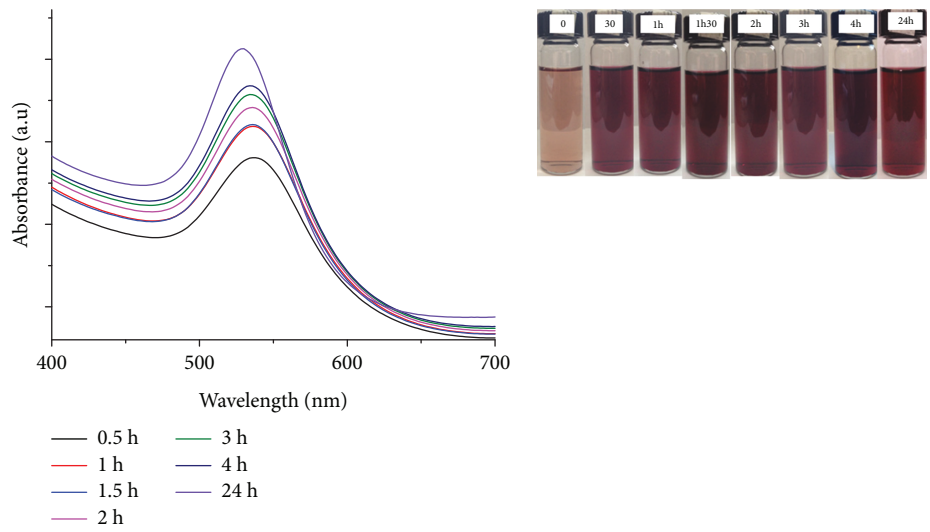

(a) (b)

Figure 1: (a) UV-Vis spectra of biogenic AuNPs measured at different times during the reaction of 0.4 mL of *Camellia sinensis* extract with 5 mL of a 10^{-3} M of $HAuCl_4$. Curve profiles correspond to 0.5 h (black), 1 h (red), 1.5 h (blue), 2 h (pink), 3 h (green), 4 h (purple), and 24 h (violet). (b) Picture of vials containing AuNPs obtained at different reaction times (0 h to 24 h).

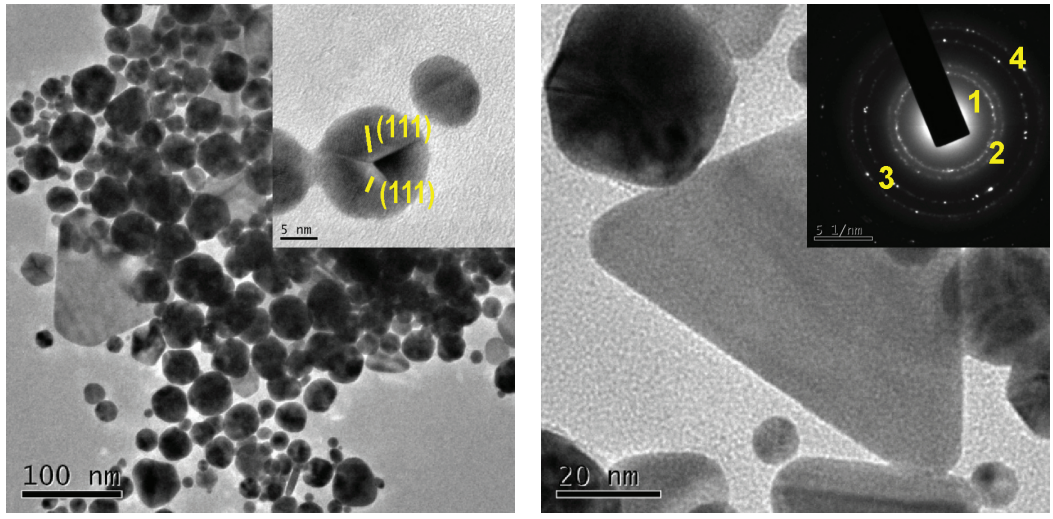

(a) (b)

Figure 2: (a, b) TEM micrographs of AuNPs obtained with 0.4 mL of *Camellia sinensis* extract. Inset in (a): HRTEM micrograph of biogenic AuNPs obtained with 0.4 mL of *Camellia sinensis* extract. Inset in (b): SAED pattern of biogenic AuNPs collected after 24 h of reaction using 0.4 mL of *Camellia sinensis* extract.

correspond to hydrocarbon skeletons of the biomolecules in green tea, while all the rest of the bands remain the same in both spectra (Figures 3(a) and 3(b)). The band due to C-O stretching at 1323 cm^{-1} is weaker on the AuNP spectrum, and the one due to torsion out of the plane of the carboxyl dimer at 960–875 cm^{-1} on the AuNP spectra exhibits significant changes [17–19]. By these observations, we can assume that the polyphenolic biomolecules present in the *Camellia sinensis* extract are responsible for the reduction of Au ions, and also, they can act as capping or passivating agents to generate the nanostructures.

3.2. Colorimetric Sensing Using AuNPs. This method of detection is a simple, sensitive, sometimes selective, rapid, and portable; complies with green chemistry principles; and can be used with a wide range of analytes. Colorimetric assays are based on the colloidal solution color change, which happens when the NPs switch from dispersed to aggregated particles (Figure 4(c)). These aggregates are mediated by certain analytes, such as metal ions. The biomolecules present on the surface of the AuNPs, in this case carboxylic groups of the capping agents, form aggregates with the metal ions by means of metal-ligand interactions,

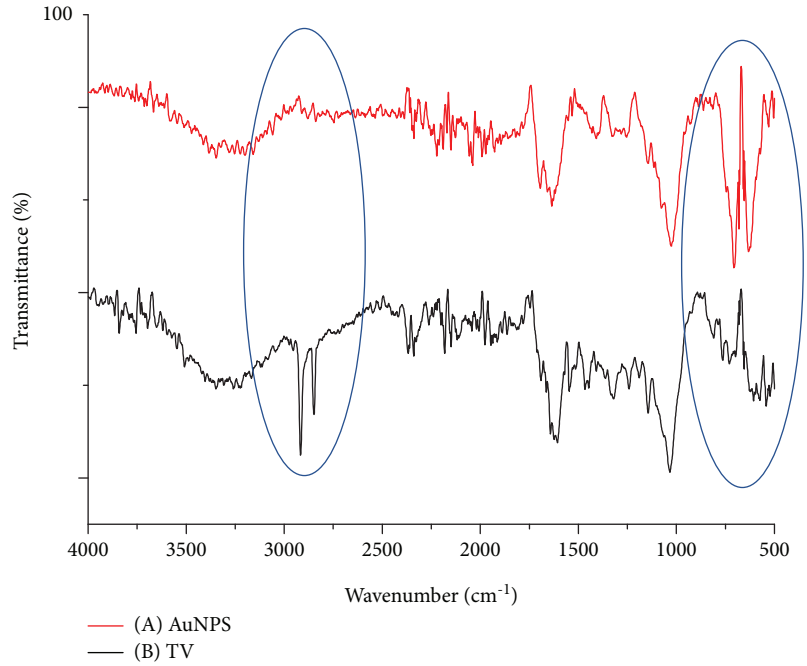

FIGURE 3: (a) FTIR spectrum of AuNPs obtained with 0.4 mL of *Camellia sinensis* extract and 5 mL of 10^{-3} M of $HAuCl_4$. (b) FTIR spectrum of *Camellia sinensis* extract.

better known as complex formation (Figure 4(b)), causing thus a color change in the AuNP colloidal solution.

The addition of the different divalent metal ions (Mg^{2+}, Hg^{2+}, Sr^{2+}, Pb^{2+}, Ca^{2+}, Cu^{2+}, and Zn^{2+}) to the AuNP colloidal solution, obtained with 0.4 mL of *Camellia sinensis* extract, had a visible color change from pink to purple-grayish (Figure 4(c)) particularly with four different metal ions: Zn^{2+}(2), Sr^{2+}(3), Ca^{2+} (7), and Cu^{2+}(8). The color change that occurs in the solution is due to the switch from individual state to aggregates, in this case is mediated by specific metal ions (Figure 4(c)) [24, 34]. This is an interesting result, since all the metals here used have similar complexing behavior [35]. Therefore, no matter the similarities in the ionic radii of the metal ions studied: Mg^{2+} (72 pm), Ca^{2+} (100 pm), Sr^{2+} (118 pm), Cu^{2+} (73 pm), Zn^{2+} (74 pm), Hg^{2+} (102 pm), and Pb^{2+} (119 pm), it seems that Mg^{2+}, Hg^{2+}, and Pb^{2+} cannot form complexes with the AuNPs as easy as the other metal ions; so, the formation of complexes, and subsequent aggregation of AuNPs, can be attributed to the chemical affinity, through electrostatic interactions, of the moieties in the biomolecules surrounding the AuNPs towards the corresponding metal ions.

3.3. Plasmon Resonance Sensing. The polyphenolic compounds present on the plant extract, such as caffeine, epicatechin, and benzoic acid, are known to form complexes with heavy metal ions in addition to transition metal cations. Some metal cations preferentially bind with the phenolic groups of the biomolecules [16]. Thus, the addition of the different metal ions employed: Mg^{2+}, Hg^{2+}, Sr^{2+}, Pb^{2+}, Ca^{2+}, Cu^{2+}, and Zn^{2+}, to the AuNP solution resulted in a bathochromic shift in the plasmon resonance, from 529 to 539 nm with Zn^{2+}, from 529 to 540 nm with Sr^{2+}, from 529 to 548 nm with Pb^{2+}, from 529 to 544 nm with Ca^{2+}, and from 529 to 558 nm with Cu^{2+} (Figure 4(a)). The extent of the shift depends on the concentration of the ions in the AuNP solution [16]. The shift in the plasmon resonance absorption band and the visual color change of the solution (Figures 4(a) and 4(b)) can be attributed to the formation of aggregates of the NPs in the presence of metal cations. To confirm the presence of aggregates, TEM studies were carried out with the AuNPs only and with AuNP metal ions (Sr^{2+}, Pb^{2+}, Ca^{2+}, Cu^{2+}, and Zn^{2+}) (Figure 4(c)). AuNPs are dispersed in the absence of metal ions (Figure 4(b), image 1), whereas, in the presence of metal ions, formation of the aggregates can be observed (Figure 4(b), images 2, 3, 7, and 8). So, the complexation of the metal ions with the phenolic hydroxyl groups present in the surface of the NPs can bring the Au particles close together. This proximity induces the coupling of the plasmon resonance resulting thus in a bathochromic shift.

In our previous article on this topic [36], AuNPs were synthesized by using *Citrus paradisi* (grapefruit) extract as a bioreducing agent. These nanoparticles possessed a unique ability to detect by plasmon resonance sensing: Hg^{2+}, Ca^{2+}, and Zn^{2+}. However, in this actual work, the AuNPs, synthesized with *Camelia sinensis* (green tea), could detect, in addition, two very important divalent metal ions: Cu^{2+} and Pb^{2+} ions by LSPR. Hence, this comparison of sensing results evidences that the chemical nature of the biomolecules surrounding the biogenic AuNPs is a key factor in the plasmonic sensing and selectivity of divalent-aqueous metal ions.

3.3.1. Sensibility Studies. To know the sensibility effect of the biogenic AuNPs obtained with 0.4 mL of *Camellia sinensis*

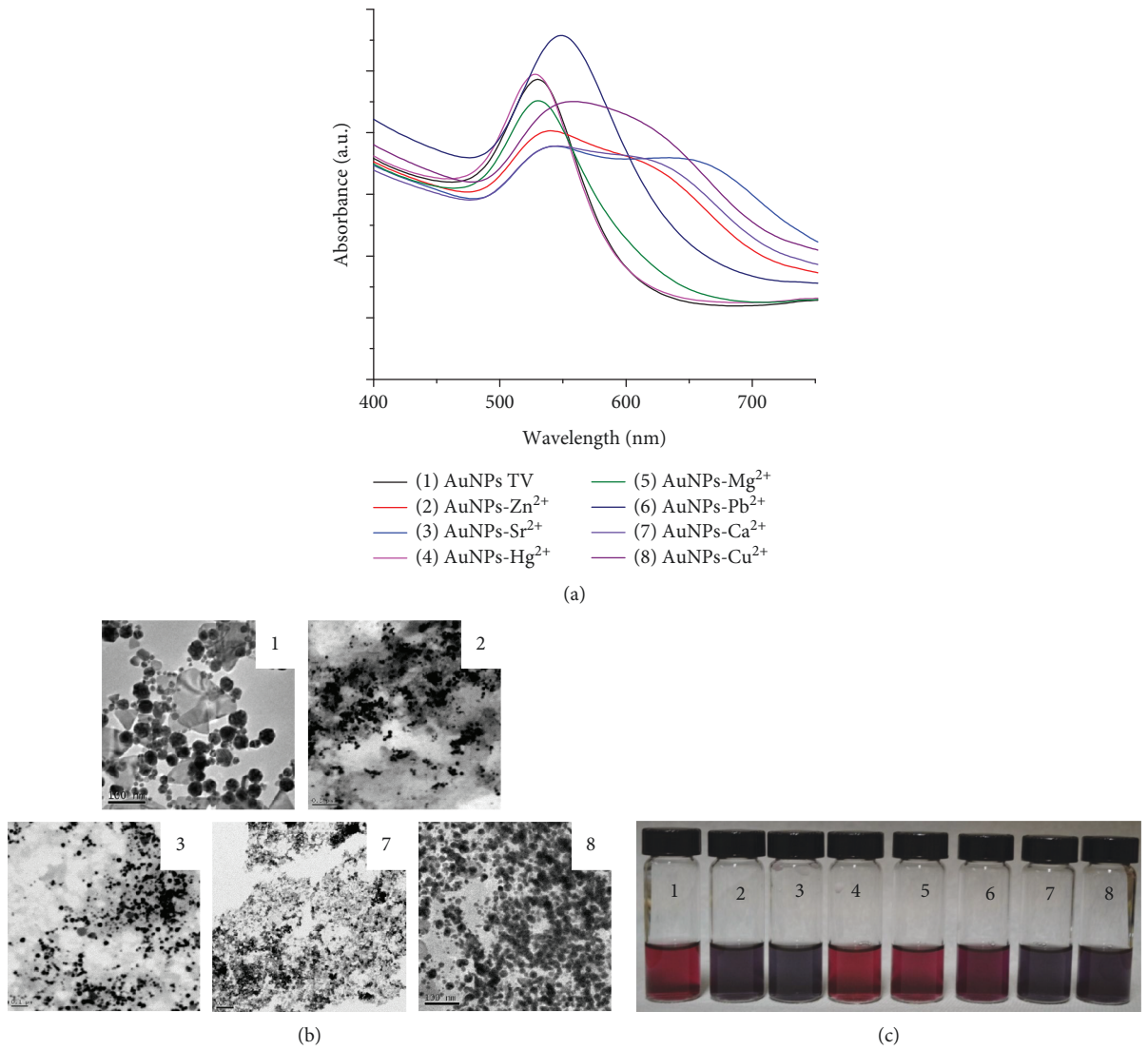

FIGURE 4: (a) UV-Vis spectra of biogenic AuNPs (synthesized with 5 mL of a 10^{-3} M $HAuCl_4$ solution and 0.4 mL of *Camellia sinensis* extract) interacting with Mg^{2+}, Hg^{2+}, Sr^{2+}, Pb^{2+}, Ca^{2+}, Cu^{2+}, and Zn^{2+} metal ions. (b) TEM images of (1) AuNPs, (2) AuNPs-Zn^{2+}, (3) AuNPs-Sr^{2+}, (7) AuNPs-Ca^{2+}, and (8) AuNPs-Cu^{2+}. (c) Picture of vials having AuNPs (synthesized with 5 mL of a 10^{-3} M HAuCl4 solution and 0.4 mL of *Camellia sinensis* extract) and the different metal ions probed, respectively.

extract towards Ca^{2+}, Cu^{2+}, Sr^{2+}, and Zn^{2+} metal ions, solutions of these metals, with concentrations from 10^{-3} to 10^{-6} M, were added to the AuNP solutions [16, 26, 31]. The degree of the bathochromic shift of the LSPR depends on the concentration of the metal ions in the NP solution [16]. When 10^{-3} M metal ion solutions were added to the colloidal AuNPs, there were bathochromic shifts of the plasmon resonance: 12 nm, from 534 to 546, for Ca^{+2} (Figure 5(a)); 15 nm, from 534 to 549 nm, for Cu^{2+}(Figure 5(b)); 8 nm, from 534 to 542 nm, for Sr^{2+} (Figure 5(c)); and 10 nm, from 534 to 544 nm, for Zn^{2+} (Figure 5(d)).

For all cases, as the metal concentration decreases below 10^{-3} M, no significant shifts were observed. Consequently, it seems that when these metal ion concentration is in the order of 10^{-3} M, aggregates of AuNPs are formed more readily, throughout complexation with these metal ions, resulting in a smaller interparticle gap and therefore greater bathochromic shifts in the plasmon resonance.

3.4. Synthesis and Characterization of Biocomposites (AuNPs/Cellulose). Au nanoparticles were synthesized by the addition of 0.4 mL of *Camellia sinensis* extract to a $HAuCl_4$ solution 10^{-3} M, as described in Experiments. After immersion of the cellulosic material into the Au colloidal solution, its white color turns into purple (Figure 6(b)), which is associated with the plasmon absorption response of the Au nanoparticles supported on the cellulosic substrate, as confirmed by the DRS UV-Vis spectrum in Figure 6(a).

Direct assembly of metal nanoparticles on cellulose substrate is promoted via electrostatic interaction between the nanoparticles and substrate. The electrostatic deposition of metal nanoparticles has been proved successfully to anchor

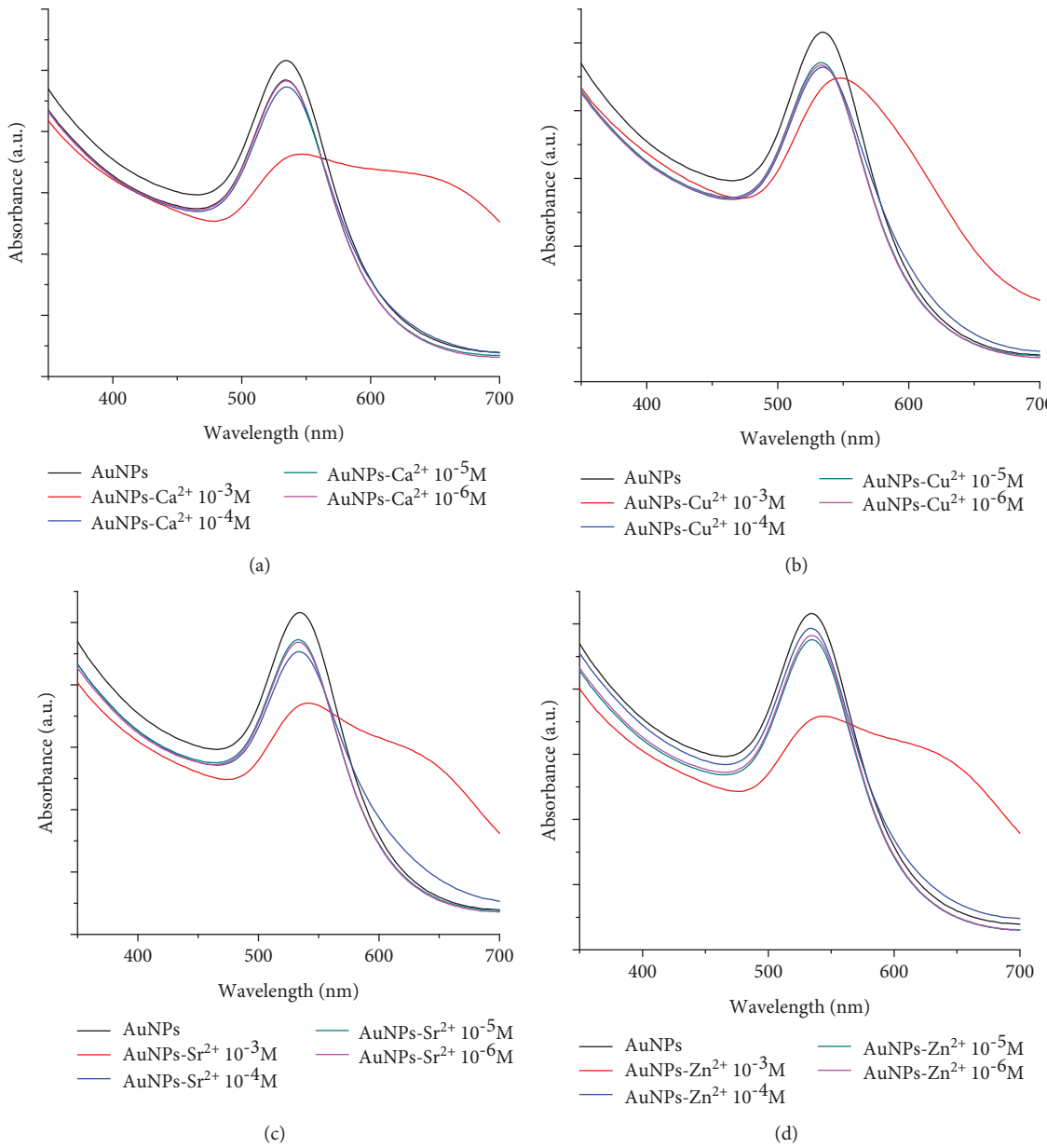

FIGURE 5: Absorption spectra changes of AuNPs upon addition of increasing concentrations, from 10^{-3} to 10^{-6} M of (a) Ca^{2+}, (b) Cu^{2+}, (c) Sr^{2+}, and (d) Zn^{2+}.

metal nanoparticles onto natural cellulose fibers [37–40] In this case, the formation of the Au/biocomposite can be explained by the self-assembling of Au nanoparticles (positively charged) and the negatively charged functional groups of the cellulose (-OH group).

The presence of the Au nanoparticles supported on cellulosic fibers is observed in the FESEM micrographs in Figure 7. EDS spectrum (Figure 7, inset) shows the existence of Au nanoparticles on the surface of the cellulosic fibers, which are uniformly distributed, as confirmed by the chemical mapping in Figure 7, indicating thus the effectiveness of the assembly of the Au nanoparticles on the cellulosic support. The deposition of Au nanoparticles on the surface of the natural cellulose material was demonstrated via electrostatic assembly. Au-decorated fibers were immersed into 1 mL of 10^{-3} M solutions of Mg^{2+}, Hg^{2+}, Sr^{2+}, Pb^{2+}, Ca^{2+}, Cu^{2+}, and Zn^{2+} ions, to evaluate the sensibility performance. The specimens were imaged using FESEM, as can be observed in Figure 8. Well-dispersed Au-nanoparticles were found to pack on the fiber surface, which do not present any morphological change after the immersion into the ion solutions. However, any visible color change was released after the contact with metallic ions. Energy-dispersive X-ray spectroscopy studies (spectra and chemical mapping) [41], presented in Figure 8, were collected for each specimen. The presence of the metal ion signal, with a homogeneous distribution around all the Au/biocomposite, is evident, indicating the retention of the metal ions. This suggests that, even

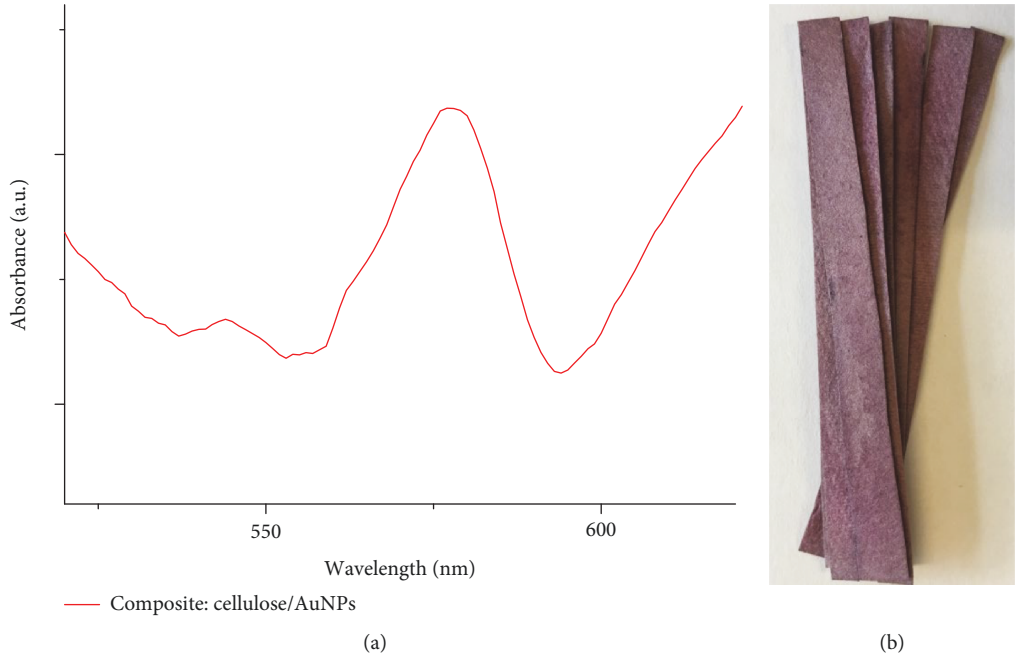

Figure 6: (a) DRS UV-Vis spectrum of the cellulosic support decorated with Au nanoparticles. (b) Picture of Au/cellulosic material composites obtained using 0.4 mL of *Camellia sinensis* aqueous extract.

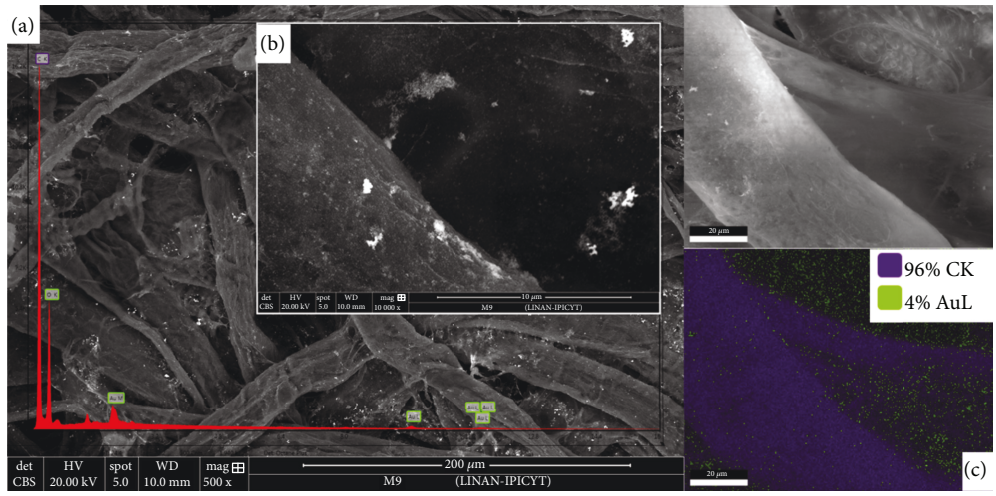

Figure 7: FESEM images at different magnifications (a, b) of the surface of cellulosic fibers coated with Au biogenic nanoparticles. The inset shows the EDS spectrum collected in (b). (c) Elemental mapping of the Au/biocomposite showing the distribution of Au nanoparticles.

though the Au/biocomposite cannot be used as a naked-eye detector for metal ions, it certainly can be considered a functional material to be employed to remove metal ions from aqueous solutions.

4. Conclusion

In summary, we have developed a simple, sensitive, and to some extent selective, colorimetric, and plasmonic sensor for divalent metal ions in aqueous solution based on biogenic and unmodified AuNps prepared with green tea as the reducing and passivating agent. This dual AuNP colloidal sensor worked very well for colorimetric detection of Ca^{2+}, Sr^{2+}, Cu^{2+}, and Zn^{2+} and also as a plasmon resonance sensor for these same metal ions, mainly. The no detection of metal ions such as Mg^{2+}, Hg^{2+}, and Pb^{2+}, which have complex characters and ionic radii similar to the ones detected, seems to be more a situation of chemical affinity of the biomolecules surrounding the AuNPs towards the different metal ions. Sensibility studies demonstrate that a 10^{-3} M solution of Ca^{2+}, Sr^{2+}, Cu^{2+}, and Zn^{2+} is optimal for the sensing of these ions. Lower concentrations preclude the formation of complexes between AuNPs and metal ions, switching off thus naked-eye and plasmon resonance sensing. Further studies are underway regarding the limit of minimum concentration detectable. Moreover, solid

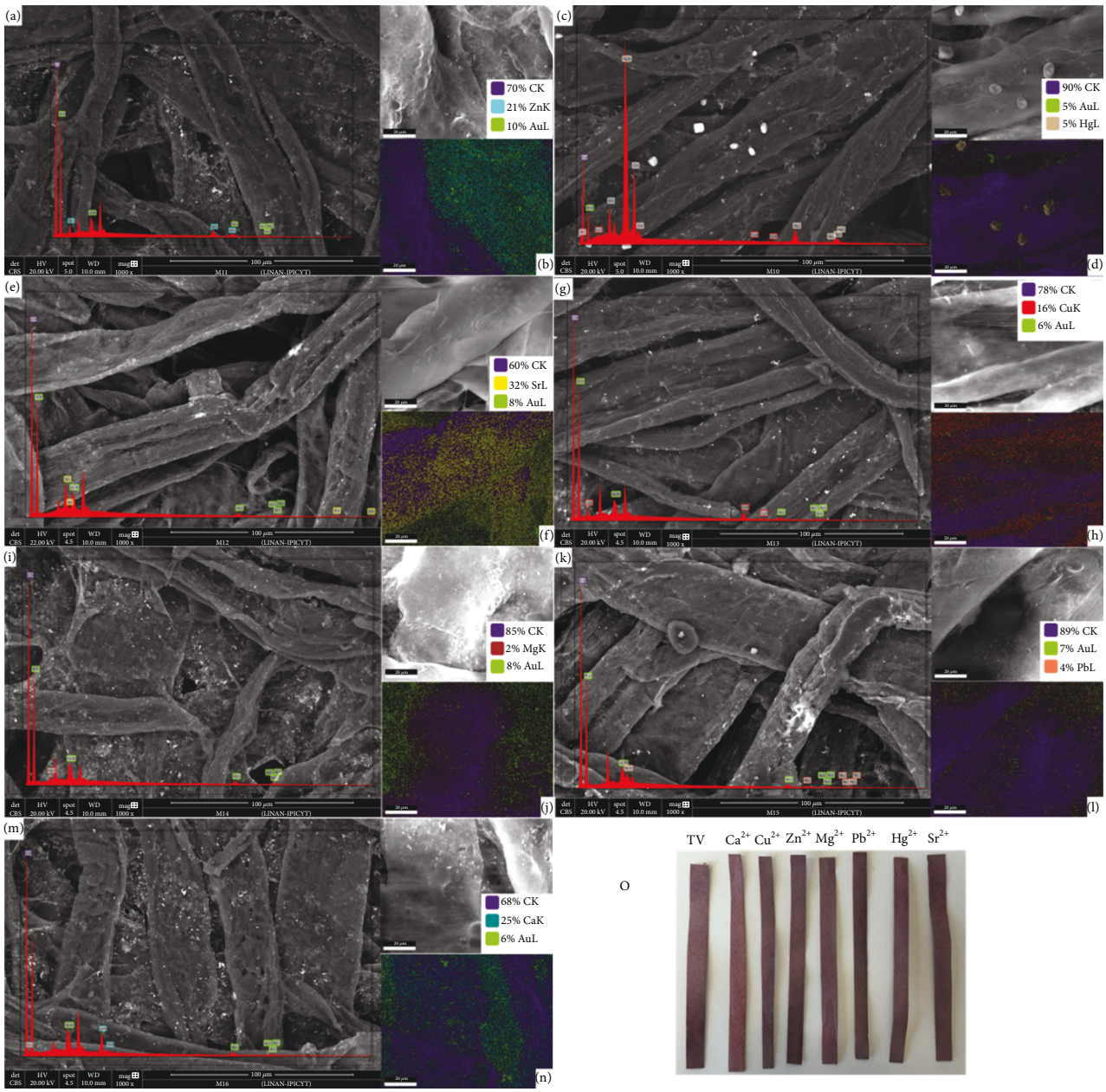

FIGURE 8: FESEM micrographs, electron dispersive X-ray spectra, and chemical mapping of the Au/biocomposite after the contact with metal ions: Zn^{2+} (a, b), Hg^{2+} (c, d), Sr^{2+} (e, f), Cu^{2+} (g, h), Mg^{2+} (i, j), Pb^{2+} (k, l), and Ca^{2+} (m, n), respectively. (o) Picture of the cellulosic material coated with Au nanoparticles after interaction with the different metal ion solutions.

biogenic AuNPs/cellulosic biocomposites were obtained with a simple in situ dip-coating methodology, expecting to get portable, fast, and reliable colorimetric sensors; nonetheless, these biocomposites resulted to have better functionalities as materials for adsorption of metal ions in an aqueous medium rather than metal ion sensors.

Data Availability

The experimental data used to support the findings of this study are included within the article.

Conflicts of Interest

The authors declare that they have not conflicts of interest.

Acknowledgments

This work was supported by CONACYT (Grant no. 280518). The authors are grateful to Lizbeth Triana-Cruz from CCIQS UAEM-UNAM, for the FTIR analyses. The authors thank Ana Iris Peña Maldonado from the Nanoscience and Nanotechnology Research National Laboratory (LINAN) at

IPICyT, for the FESEM characterization. LESD thanks CONACYT for the scholar Grant no. 373046.

References

[1] G. Aragay, J. Pons, and A. Merkoçi, "Recent trends in macro-, micro-, and nanomaterial-based tools and strategies for heavy-metal detection," *Chemical Reviews*, vol. 111, no. 5, pp. 3433–3458, 2011.

[2] H. Ramsurn and R. B. Gupta, "Nanotechnology in solar and biofuels," *ACS Sustainable Chemistry & Engineering*, vol. 1, no. 7, pp. 779–797, 2013.

[3] K. Savolainen, H. Alenius, H. Norppa, L. Pylkkänen, T. Tuomi, and G. Kasper, "Risk assessment of engineered nanomaterials and nanotechnologies-a review," *Toxicology*, vol. 269, no. 2-3, pp. 92–104, 2010.

[4] J. Y. Song, H. K. Jang, and B. S. Kim, "Biological synthesis of gold nanoparticles using Magnolia kobus and Diopyros kaki leaf extracts," *Process Biochemistry*, vol. 44, no. 10, pp. 1133–1138, 2009.

[5] Y. Cheun Yeh, B. Creran, and V. M. Rotello, "Gold nanoparticles: preparation, properties, and applications in bionanotechnology," *Nanoscale*, vol. 4, no. 6, pp. 1871–1880, 2012.

[6] B. RoÂżalska, B. Sadowska, A. Budzyńska, P. Bernat, and S. RoÂżalska, "Biogenic nanosilver synthesized in *Metarhizium robertsii* waste mycelium extract–as a modulator of *Candida albicans* morphogenesis, membrane lipidome and biofilm," *PLoS One*, vol. 13, no. 3, article e0194254, 2018.

[7] M. Annadhasan, T. Muthukumarasamyvel, V. R. Sankar Babu, and N. Rajendiran, "Green synthesized silver and gold nanoparticles for colorimetric detection of Hg^{2+}, Pb^{2+}, and Mn^{2+} in aqueous medium," *ACS Sustainable Chemistry & Engineering*, vol. 2, no. 4, pp. 887–896, 2014.

[8] C. Noguez, "Optical properties of isolated and supported metal nanoparticles," *Optical Materials*, vol. 27, no. 7, pp. 1204–1211, 2005.

[9] C. Noguez, "Surface plasmons on metal nanoparticles: the influence of shape and physical environment," *The Journal of Physical Chemistry C*, vol. 111, no. 10, pp. 3806–3819, 2007.

[10] K. M. Mayer and J. H. Hafner, "Localized surface plasmon resonance sensors," *Chemical Reviews*, vol. 111, no. 6, pp. 3828–3857, 2011.

[11] M. Grzelczak and L. M. Liz-Marzán, "Colloidal nanoplasmonics: from building blocks to sensing devices," *Langmuir*, vol. 29, no. 15, pp. 4652–4663, 2013.

[12] J. N. Anker, W. P. Hall, O. Lyandres, N. C. Shah, J. Zhao, and R. P. Van Duyne, "Biosensing with plasmonic nanosensors," *Nature Materials*, vol. 7, no. 6, pp. 442–453, 2008.

[13] J. Langer, S. M. Novikov, and L. M. Liz-Marzán, "Sensing using plasmonic nanostructures and nanoparticles," *Nanotechnology*, vol. 26, no. 32, article 322001, 2015.

[14] I. Fratoddi, A. Cartoni, I. Venditti et al., "Gold nanoparticles functionalized by rhodamine B isothiocyanate to tune plasmonic effects," *Journal of Colloid and Interface Science*, vol. 513, pp. 10–19, 2018.

[15] E. Priyadarshini and N. Pradhan, "Gold nanoparticles as efficient sensors in colorimetric detection of toxic metal ions: a review," *Sensors and Actuators B*, vol. 238, pp. 888–902, 2017.

[16] K. Yoosaf, B. Itty Ipe, C. H. Suresh, and K. George Thomas, "In situ synthesis of metal nanoparticles and selective naked-eye detection of lead ions from aqueous media," *The Journal of Physical Chemistry C*, vol. 111, no. 34, pp. 12839–12847, 2007.

[17] T. M. Rababah, N. S. Hettiarachchy, and R. Hora, "Total phenolics and antioxidant activities of fenugreek, green tea, black tea, grape seed, ginger, rosemary, gotu kola, and ginkgo extracts, vitamin E, and tert-butylhydroquinone," *Journal of Agricultural and Food Chemistry*, vol. 52, no. 16, pp. 5183–5186, 2004.

[18] Y. Y. Loo, B. W. Chieng, M. Nishibuchi, and S. Radu, "Synthesis of silver nanoparticles by using tea leaf extract from Camellia sinensis," *International Journal of Nanomedicine*, vol. 7, pp. 4263–4267, 2012.

[19] P. O. Owuor and M. Obanda, "The use of green tea (Camellia sinensis) leaf flavan-3-ol composition in predicting plain black tea quality potential," *Food Chemistry*, vol. 100, no. 3, pp. 873–884, 2007.

[20] K. Saha, S. S. Agasti, C. Kim, X. Li, and V. M. Rotello, "Gold nanoparticles in chemical and biological sensing," *Chemical Reviews*, vol. 112, no. 5, pp. 2739–2779, 2012.

[21] C. Wang and C. Yu, "Detection of chemical pollutants in water using gold nanoparticles as sensors: a review," *Reviews in Analytical Chemistry*, vol. 32, no. 1, pp. 1–14, 2013.

[22] P. D. Howes, R. Chandrawati, and M. M. Stevens, "Colloidal nanoparticles as advanced biological sensors," *Science*, vol. 346, no. 6205, article 1247390, 2014.

[23] L. Polavarapu, J. Pérez-Juste, H. X. Qi, and L. M. Liz-Marzán, "Optical sensing of biological, chemical and ionic species through aggregation of plasmonic nanoparticles," *The Journal of Materials Chemistry C*, vol. 2, no. 36, p. 7460, 2014.

[24] X. Li, Y. Tang, X. Cao, D. Lu, F. Luo, and W. Shao, "Preparation and evaluation of orange peel cellulose adsorbents for effective removal of cadmium, zinc, cobalt and nickel," *Colloids and Surfaces A: Physicochemical and Engineering Aspects*, vol. 317, no. 1-3, pp. 512–521, 2008.

[25] M. A. Momodu and C. A. Anyakora, "Heavy metal contamination of ground water: the Surulere case study," *Research Journal Environmental and Earth Sciences.*, vol. 2, no. 1, pp. 39–43, 2010.

[26] C. Joseph Kirubaharan, D. Kalpana, Y. S. Lee et al., "Biomediated silver nanoparticles for the highly selective copper(II) ion densor applications," *Industrial & Engineering Chemistry Research*, vol. 51, no. 21, pp. 7441–7446, 2012.

[27] P. Prosposito, F. Mochi, E. Ciotta et al., "Hydrophilic silver nanoparticles with tunable optical properties: application for the detection of heavy metals in water," *Beilstein Journal of Nanotechnology*, vol. 7, pp. 1654–1661, 2016.

[28] E. Priyadarshini and N. Pradhan, "Metal-induced aggregation of valine capped gold nanoparticles: an efficient and rapid approach for colorimetric detection of Pb^{2+} ions," *Scientific reports*, vol. 7, no. 1, article 9278, 2017.

[29] S. Kaviya and E. Prasad, "Sequential detection of Fe^{3+} and As^{3+} ions by naked eye through aggregation and disaggregation of biogenic gold nanoparticles," *Analytical Methods*, vol. 7, no. 1, pp. 168–174, 2015.

[30] L. Polavarapua and L. M. Liz-Marzán, "Towards low-cost flexible substrates for nanoplasmonic sensing," *Physical Chemistry Chemical Physics*, vol. 15, no. 15, pp. 5288–5300, 2013.

[31] L. E. Silva De Hoyos, V. Sánchez Mendieta, A. R. Vilchis Nestor, and M. A. Camacho López, "Biogenic silver nanoparticles as sensors of Cu^{2+} and Pb^{2+} in aqueous solutions," *Universal Journal of Materials Science*, vol. 5, no. 2, pp. 29–37, 2017.

[32] C. H. Coyle, B. J. Philips, S. N. Morrisroe, M. B. Chancellor, and N. Yoshimura, "Antioxidant effects of green tea and its polyphenols on bladder cells," *Life Sciences*, vol. 83, no. 1-2, pp. 12–18, 2008.

[33] M. Chen, H. Kang, Y. Gong, J. Guo, H. Zhang, and R. Liu, "Bacterial cellulose supported gold nanoparticles with excellent catalytic properties," *ACS Applied Materials & Interfaces*, vol. 7, no. 39, pp. 21717–21726, 2015.

[34] F. Mochi, L. Burratti, I. Fratoddi et al., "Plasmonic sensor based on interaction between silver nanoparticles and Ni^{2+} or Co^{2+} in water," *Nanomaterials*, vol. 8, no. 7, p. 488, 2018.

[35] I. V. Pletnev and V. V. Zernov, "Classification of metal ions according to their complexing properties: a data-driven approach," *Analytica Chimica Acta*, vol. 455, no. 1, pp. 131–142, 2002.

[36] L. E. Silva-De Hoyos, V. Sánchez-Mendieta, M. A. Camacho-López, J. Trujillo-Reyes, and A. R. Vilchis-Néstor, "Plasmonic and fluorescent sensors of metal ions in water based on biogenic gold nanoparticles," *Arabian Journal of Chemistry*, 2018, https://doi.org/10.1016/j.arabjc.2018.02.016.

[37] S. K. Mahadeva, K. Walus, and B. Stoeber, "Paper as a platform for sensing applications and other devices: a review," *ACS Applied Materials & Interfaces*, vol. 7, no. 16, pp. 8345–8362, 2015.

[38] J. He, T. Kunitake, and A. Nakao, "Facile in situ synthesis of noble metal nanoparticles in porous cellulose fibers," *Chemistry of Materials*, vol. 14, pp. 4401–4406, 2003.

[39] D. Patiño-Ruiz, L. Sanchez-Botero, J. Hinestroza, and A. Herrera, "Modification of cotton fibers with magnetite and magnetic core-shell mesoporous silica nanoparticles," *Physica Status Solidi A: Applications and Materials Science*, vol. 215, no. 19, 2018.

[40] H. Dong and J. P. Hinestroza, "Metal nanoparticles on natural cellulose fibers: electrostatic assembly and in situ synthesis," *ACS Applied Materials & Interfaces*, vol. 1, no. 4, pp. 797–803, 2009.

[41] S. Rades, V.-D. Hodoroaba, T. Salge et al., "High-resolution imaging with SEM/T-SEM, EDX and SAM as a combined methodical approach for morphological and elemental analyses of single engineered nanoparticles," *RSC Advances*, vol. 4, no. 91, pp. 49577–49587, 2014.